JOURNAL OF MATERIALS SCIENCE 10 (1975) 101–108

Evidence for the existence of faulting in a splat-cooled δ-Pu (Ti) alloy

R. B. ROOF, R. O. ELLIOTT
University of California, Los Alamos Scientific Laboratory, Los Alamos, New Mexico, USA

Examination of X-ray diffraction profiles of a "splat-cooled" 15 Ti–85 Pu alloy has revealed that the material contains a large amount of twinning coupled with a reasonably small crystallite size and high strain. The localized strain is estimated to be 0.6%, the crystallite size ≅250 Å, and the twinning fault probability is large at 0.043.

1. Introduction

Metastable ε-Pu (bcc) solid solutions were recently retained to room temperature for the first time by splat-cooling* Pu-rich Pu–Ti alloys from the melt [1]. Alloy compositions were in the range from ~20 to more than 45 at. % Ti. Metastable δ-Pu (fcc) solid solutions were also retained to room temperature in alloys containing lesser amounts of Ti. The X-ray diffraction patterns of these δ-alloys showed strong peak broadening that increased with increasing Ti content and varied considerably for different hkl sets within each pattern [1]. The purpose of the present work was to characterize one such δ-alloy on an atomic scale with regard to crystallite size, lattice strain, and various lattice stacking faults. The alloy under consideration contained 85 at. % Pu plus 15 at. % Ti and was fcc with $a_0 = 4.558$ Å†. The 111, 200, 220, 311 and 222 reflections were available for examination.

Examination of the shape of an X-ray diffraction profile is a technique whereby information can be obtained concerning the condition of the material on an atomic scale. Crystallite size, lattice strain, and lattice stacking faults are items that can be obtained. Since description of the general procedures usually employed are available in standard literature references [2-5] the detailed procedures will not be described further in this paper. A computer program, UNFOLD, was written to aid in the Fourier analysis of the peak shape. A unique feature of this program is the inclusion of equations due to Wilson [6, 7] to calculate standard deviations of the Fourier coefficients directly in terms of the experimental intensity expressed as counts per second. The standard deviations were further propagated (with co-variance included) through the complex division necessary to arrive at Fourier coefficients free from instrumental abberations.

For the alloy under examination, the reflections 111 and 222 are quite sharp and 200, 220, 311 are relative broad. Typical experimental patterns taken with Cu$K\alpha$ radiation are shown in Figs. 1 and 2. A fine-grained well-annealed aluminium specimen was used as the reference material to measure instrumental abberations. The Al 111 line was used as the reference line for the alloy 111 and 200 lines with the Al 220 line being the reference for the alloy 220, 311, and 222 lines. Complex division of the alloy line profiles by the reference line profiles is termed unfolding and results in Fourier coefficients free from instrumental effects. These unfolded coefficients may be used to resynthesize line profiles from which crystallite size, strain, and stacking faults can be obtained. Two resynthesized profiles are shown in Figs. 3 and 4.

There are generally three methods used for the analysis of line profiles; the obtaining of the integral breadth of the line profile, the examination of the Fourier coefficients describing the shape of the line, and the evaluation of the

*The term "splat-cooling" refers to one of a variety of different techniques for rapid quenching of alloy melts. A necessary requirement in all splat-cooling techniques is to generate thin liquid films in perfect contact with a good thermal conductor, such as copper or silver.

†There is a misprint in [1] where the lattice parameter is given as 4.588 Å.

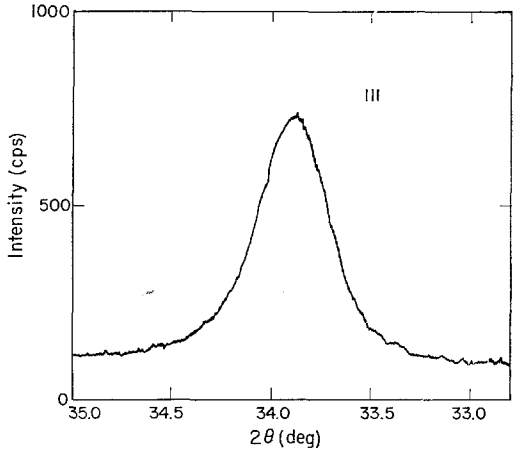

Figure 1 Experimental X-ray diffraction profile of the 111 reflection of a 15Ti–85Pu splat-cooled alloy.

second moment of the line profile about its centroid. Each of these methods will be discussed in turn below.

2. Data analysis

2.1. Integral breadth

The integral breadth of a line profile may be found in two ways. It is convenient to least-squares fit a Gaussian curve with a polynomial background to the data [8]. From this fit the integral breadth is found as $\sqrt{(2\pi)}$ times the Gaussian width parameter. The second way is to divide the difference in 2θ across the line profile by the sum of the unfolded Fourier coefficients. Unless the profile is quite asymmetrical the two methods should yield comparable results. The integral breadths obtained by these methods are

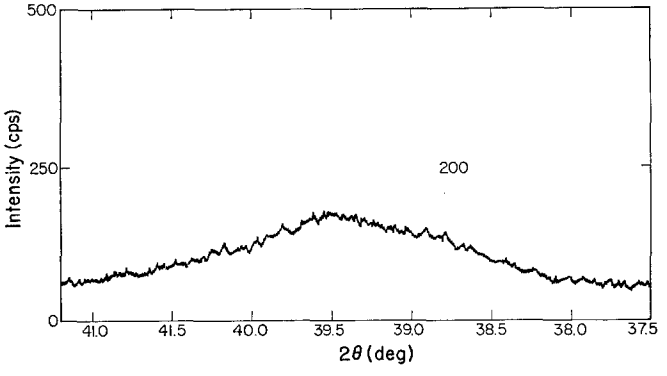

Figure 2 Experimental X-ray diffraction profile of the 200 reflection of a 15Ti–85Pu splat-cooled alloy.

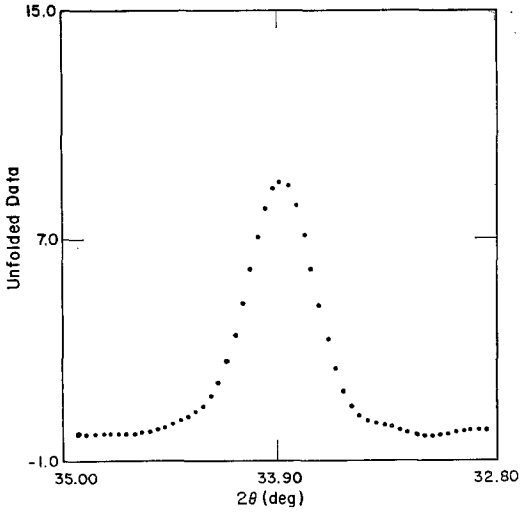

Figure 3 The 111 diffraction profile resynthesized from unfolded Fourier coefficients. Compare with Fig. 1 for the effects of instrumental abberations.

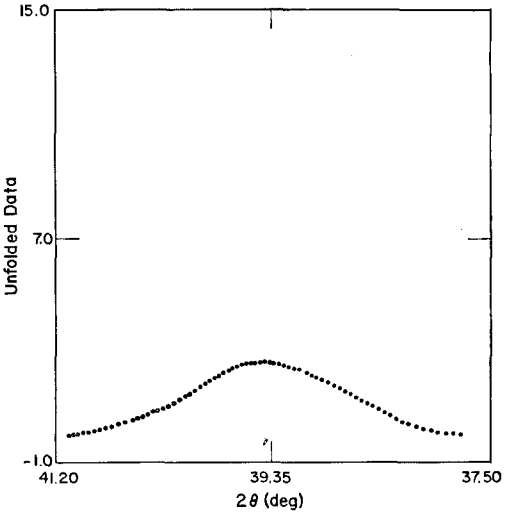

Figure 4 The 200 diffraction profile resynthesized from unfolded Fourier coefficients. Compare with Fig. 2 for the effects of instrumental abberations.

in units of degrees 2θ and are converted to units of s, $Å^{-1}$, ($s = 2 \sin\theta/\lambda$) by the multiplication of the factor $(2\pi/360) \times (\cos\theta/\lambda)$. The integral breadths, $\beta(s)$, calculated by this procedure are listed in Table I. The subscript G refers to a Gaussian fit of the data while the subscript Σ refers to the summation of Fourier coefficients.

TABLE I Experimental integral breadths, $\beta(s)$, for a splat-cooled 15Ti–85 Pu Alloy

hkl	$\beta(s)_G$ ($Å^{-1}$)	$\beta(s)_\Sigma$ ($Å^{-1}$)
111	$4.71 \pm 3 \times 10^{-3}$	$4.72 \pm 2 \times 10^{-3}$
200	17.00 ± 10	16.35 ± 12
220	13.12 ± 15	12.88 ± 13
311	15.50 ± 11	14.85 ± 19
222	6.57 ± 9	6.65 ± 11

The data of Table I are plotted in Fig. 5 as $(\beta_s)^2$ versus $\sin^2\theta/\lambda^2$. The straight line was fitted by least-squares techniques. The crystallite size,

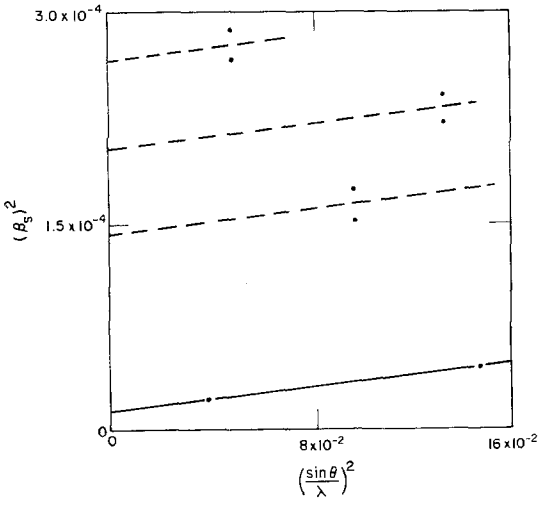

Figure 5 Experimental integral breadth for a 15Ti–85Pu splat-cooled alloy as a function of $\sin^2\theta/\lambda^2$.

D, and average strain, ϵ_I, perpendicular to the 111 planes, determined from the intercept and slope, respectively, of the straight line, are $D = 258 \pm 4$ Å, $\epsilon_I = 0.0035 \pm 1$. Second order reflections of 200, 220, and 311 are not available for examination and strain and crystallite size for these directions cannot be reliably determined. The very great departure of the integral breadth of the lines from the values for 111-222 are indications that considerable stacking faulting exists. If the assumption is made that the strain determined from the 111-222 lines is isotropic then the crystallite size perpendicular to 200, 220, and 311 is respectively 61 ± 1, 84 ± 3, and 70 ± 2 Å as determined from the intercepts of the dashed lines of Fig. 5.

2.2. Fourier coefficients

The normalized unfolded Fourier coefficients ($C = (A^2 + B^2)^{1/2}$) for the five reflections examined are plotted in Fig. 6. There are two general sets observed; those coefficients belonging to the

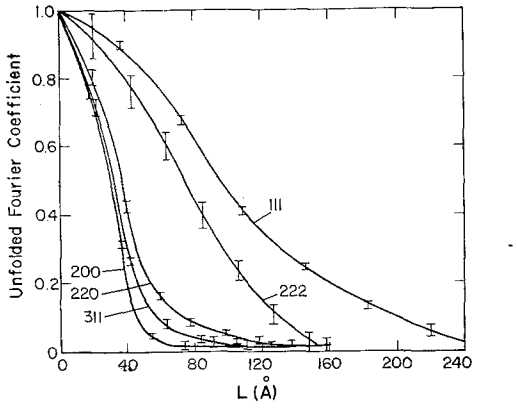

Figure 6 Normalized unfolded Fourier coefficients for five reflections from splat-cooled 15Ti–85Pu alloy.

relatively sharp lines 111, 222 and the second set belonging to the broad lines 200, 220, and 311. In Fig. 7 the Fourier coefficients are plotted as a function of $h^2 + k^2 + l^2$ for constant L, with $L = 60$ Å as a typical example. Table II lists the intercepts and slopes obtained by fitting the data to the general exponential equation $y = a \exp bx$ for selected values of L. Again, it is assumed that strain determined from 111-222

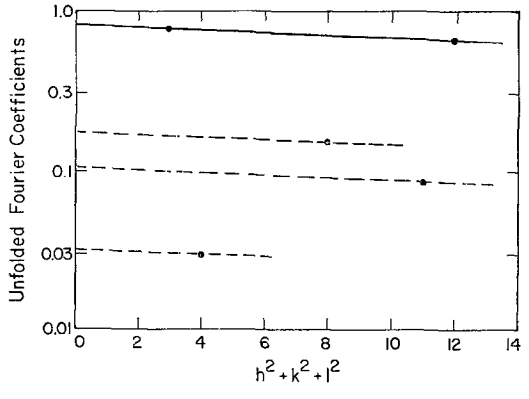

Figure 7 Logarithmic plot of normalized unfolded Fourier coefficients from splat-cooled 15Ti–85Pu for $L = 60$ Å.

TABLE II Intercepts and slopes as a function of L. Obtained by fitting data of Fig. 6 to the equation $y = a \exp bx$

L (Å)	Intercept				Slope
	111-222	200	220	311	
10	0.987	0.898	0.927	0.912	−0.002 24
20	0.962	0.753	0.827	0.775	−0.004 17
30	0.941	0.535	0.690	0.597	−0.007 49
40	0.895	0.208	0.453	0.332	−0.009 31
50	0.870	0.075	0.272	0.178	−0.015 80
60	0.821	0.033	0.178	0.108	−0.021 42
70	0.768	0.01	0.128	0.07	−0.030 90
80	0.698	0.01	0.103	0.05	−0.039 40
90	0.619	0.01	0.088	0.03	−0.048 70
100	0.549	0.01	0.064	0.03	−0.059 20
110	0.504		0.056	0.02	−0.077 00
120	0.460		0.043	0.03	−0.096 30
130	0.448				−0.133 80
140	0.450				−0.183 20

is isotropic and this fixes the constant b for the reflections 200, 220, and 311 in the exponential equation.

The root mean squared strain, ϵ_F^2, can be calculated from the slope of the Fourier coefficients curve plotted as a function of $h^2 + k^2 + l^2$ utilizing the following equation.

$$\epsilon_F^2 = \frac{a_0^2}{2\pi^2 L^2}(-\text{slope}) \qquad (1)$$

where $a_0 = 4.558$ Å for 15Ti–85Pu. The strains determined in this manner are plotted in Fig. 8 as a function of L. While the strains are in general agreement with the value determined by the integral breadth method ($\simeq 0.0035$), Fig. 8 indicates that as $L \rightarrow 0$ the local strain becomes very high indeed. This might be expected due to the cooling rates of millions of degrees per second obtainable by the splat-cooling technique. At $L = 0$ the local strain is estimated to be 0.0058 ± 3.

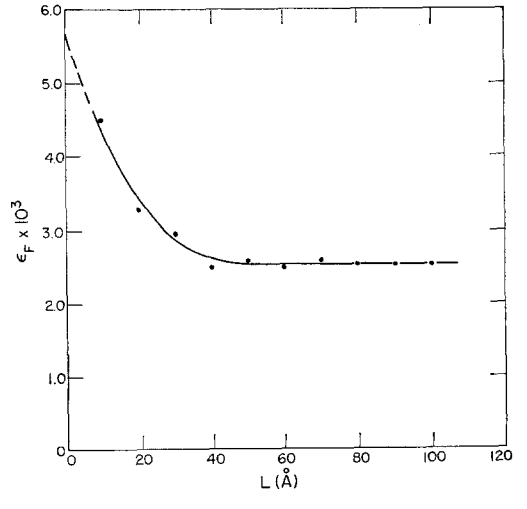

Figure 8 Variation of strain, ϵ_F, as a function of L.

The Fourier crystallite size coefficients, the intercepts of Table II, are plotted as a function of L in Fig. 9. The intersection on the L-axis of a line drawn through the linear portion of the curve yields an effective crystallite size, D_e. For the four reflections in Fig. 9, D_e is 173 ± 3 Å for 111-222, 48 ± 7 for 200, 63 ± 6 for 220, and 58 ± 5 for 311.

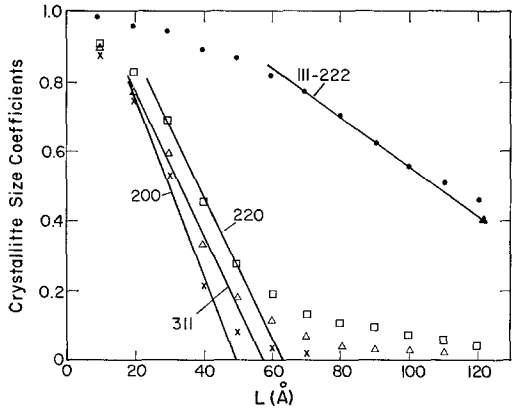

Figure 9 Crystallite size via the Fourier coefficient technique.

The separation of the true crystallite size and the compound stacking faults from the effective crystallite size is accomplished by plotting $1/D_e$ as a function of V_{hkl}. V_{hkl} is a constant for a given value of hkl and reflects the contribution to the total line profile observed of the various signed permutations of hkl that are affected by stacking faults. Tables of V_{hkl} are available [3, 4]. The intercept in Fig. 10 is the reciprocal of the true crystallite size D and the slope is equal to $(1.5\ \alpha' + 1.5\ \alpha'' + \beta)/a_0$ where α' = the probability of finding a single stacking fault between neighbouring 111 planes, α'' = the double stacking fault probability; and β = the twin fault probability. From the intercept and slope of Fig. 10; $D = 263 \pm 570$ Å and $(1.5\ \alpha' + 1.5\ \alpha'' + \beta) = 0.078 \pm 0.055$.

The sine terms, B, of the normalized unfolded. Fourier coefficients may be used to obtain

information about α'' and β according to the following formula [3, 4];

$$(B_n)_{n\to 0} = \frac{(4.5\,\alpha'' + \beta)}{\sqrt{3}} \cdot X_{hkl} \qquad (2)$$

where n = harmonic number and X_{hkl} is a constant for a given hkl and is similar in nature to V_{hkl}. Tables of X_{hkl} are available [3, 4].

A problem exists concerning the functional form of the extrapolation of the sine terms, B. As shown in Fig. 11, for example, a simple polynominal is suggested. Warren [9] has derived

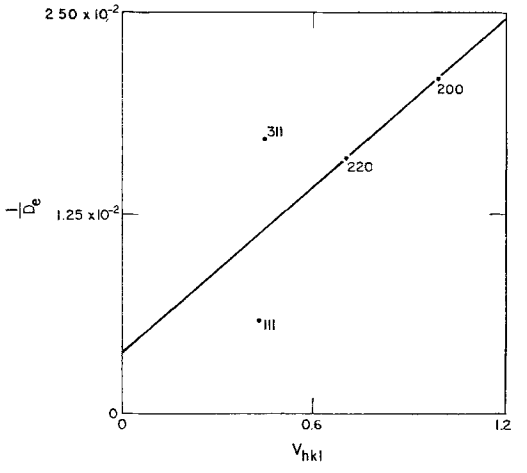

Figure 10 Separation of true crystallite size and compound stacking fault parameter from effective crystallite size.

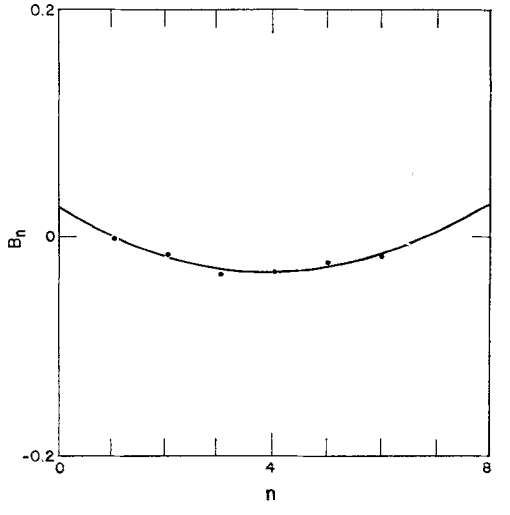

Figure 11 Variation of Fourier sine coefficients, B_n, as a function of harmonic number, n. The 111 reflection of a 15Ti–85Pu splat-cooled alloy.

the form of the following equation which is hkl dependent and predicts algebraic signs for the coefficients of the quadratic representation in L that are in general agreement with the observed data:

$$B_L{}^{hkl} = \frac{(4.5\,\alpha'' + \beta)}{\sqrt{3}(u+b)} \left\{ \sum_b \frac{(\pm) L_0}{|L_0|} - \frac{(1/N_3 + 1.5\,\alpha' + 1.5\,\alpha'' + \beta)}{a_0 h_0} \left[\sum_b (\pm) L_0 \right] L + \frac{(1.5\,\alpha' + 1.5\,\alpha'' + \beta)}{N_3 a_0{}^2 h_0{}^2} \left[\sum_b (\pm) L_0 |L_0| \right] L^2 \right\} . \qquad (3)$$

Collection of terms and introduction of abbreviations yields

$$B_L{}^{hkl} = \frac{(4.5\,\alpha'' + \beta)}{\sqrt{3}(u+b)} \left\{ \sum_b \frac{(\pm) L_0}{|L_0|} - C_1{}^{hkl} \frac{1}{h_0} \left[\sum_b (\pm) L_0 \right] L + C_2{}^{hkl} \frac{1}{h_0{}^2} \left[\sum_b (\pm) L_0 |L_0| \right] L^2 \right\} \qquad (4)$$

This may be reduced to

$$y = P_1 x_1 + P_2 x_2 + P_3 x_3 . \qquad (5)$$

P_1 is found by setting $x_1 = 1.0$ and least squares fitting data for each hkl to the variables x_2 and x_3 including the constraint of the correct algebraic sign for P_2 and P_3. P_1 is plotted as a function of X_{hkl} in Fig. 12. The slope is determined to be 0.058 ± 0.029 from which is calculated $(4.5\,\alpha'' + \beta) = 0.100 \pm 0.050$.

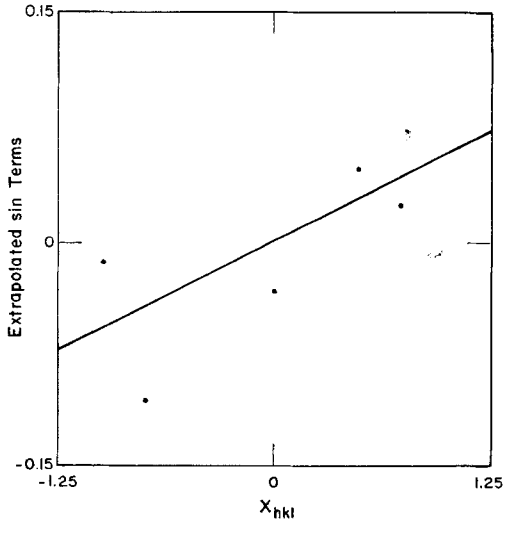

Figure 12 Variation of extrapolated Fourier coefficient sine terms as a function of X_{hkl}.

Values for two equations involving the three types of stacking faults have been obtained and a third value from a different equation is needed to separate the stacking faults. The lattice parameter, a_{hkl}, calculated from a peak position of the individual hkl reflections of fcc materials depends on the true lattice parameter a_0, the difference $(\alpha' - \alpha'')$, the residual stress σ, and the geometrical abberations of the diffractometer. It has been shown [3] that these quantities are related according to

$$a_{hkl} = a_0 + (S_1)_{hkl}{}^A \cdot \sigma \cdot a_0 + G_{hkl} \cdot a_0 \cdot (\alpha' - \alpha'') + m \cdot f(\theta) \quad (6)$$

where $(S_1)_{hkl}{}^A$ and G_{hkl} are constants which depend on the planes hkl. Tables of G_{hkl} are available [3, 4]. The second term of the equation is dependent on a combination of elastic constants and reflecting planes hkl, the residual stress and the lattice constant. After some reduction it can be expressed as

$$(S_1)_{hkl}{}^A \cdot \sigma \cdot a_0 = P_2 + P_3 \left\{ \frac{h^2k^2 + k^2l^2 + h^2l^2}{(h^2 + k^2 + l^2)^2} \right\}$$

The third term may be written as

$$G_{hkl} \cdot a_0 \cdot (\alpha' - \alpha'') = P_4 \cdot G_{hkl} \ .$$

The fourth term is

$$m \cdot f(\theta) = P_5 \cdot \cos\theta\cot\theta$$

for diffractometer focusing geometry. Equation 6 may now be represented as

$$y = P_1x_1 + P_2x_2 + P_3x_3 + P_4x_4 + P_5x_5 \ . \quad (7)$$

Values for a_{hkl} (ie. y) were calculated from 2θ values representing the centroids of the observed experimental intensity data. Corrections to 2θ for deviations from the focusing circle of the diffractometer were applied. Values for the remaining terms (ie. x_j, $j = 1, 5$) were calculated or taken from published tables [3, 4]. The x, y values are elements of a matrix and these are arranged in an array in Table III.

The data represented in Table III are usually plotted as y versus x_5 with deviations from a straight line representing the contributions of stacking faults and stress to the lattice parameter (see Fig. 13). As two columns of matrix elements are equal, x_1 and x_2, the matrix is singular and cannot be solved in this form. Since the lattice constant for this material is known ($a_0 = 4.558$) the parameter P_1 is set equal to this value and the remaining parameters were computed by least squares techniques. Their values are $P_2 = 0.0027$, $P_3 = 0.0042$, $P_4 = -0.0103$, $P_5 = 0.0021$. The positive signs for P_2 and P_3 are interpreted to mean that the material is under tensile stress. The stacking fault parameter of interest, $(\alpha' - \alpha'')$, is obtained from the ratio P_4/P_1 and equals -0.002 ± 0.008.

TABLE III Matrix elements for the solution of equation (7) for experimental values obtained for splat-cooled 15Ti–85 Pu

hkl	y (Å)	x_1	x_2	x_3	x_4	x_5
111	4.5695	1.0	1.0	0.333	−0.035	3.114
200	4.5650	1.0	1.0	0.000	0.069	2.610
220	4.5644	1.0	1.0	0.250	−0.035	1.611
311	4.5651	1.0	1.0	0.157	0.013	1.223
222	4.5639	1.0	1.0	0.333	0.017	1.119

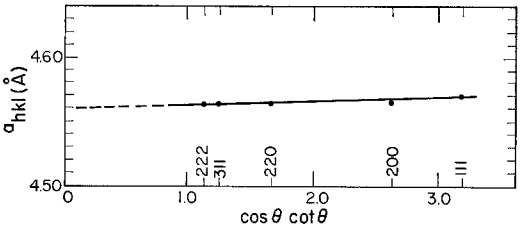

Figure 13 Calculated lattice constant, a_{hkl}, versus $\cos\theta\cot\theta$ for a sample of splat-cooled 15Ti–85Pu.

Separation of stacking fault probabilities is accomplished by solving the following equations:

$$\begin{aligned} 1.5\alpha' + 1.5\alpha'' + \beta &= 0.078 \pm 0.055 \\ 4.5\alpha'' + \beta &= 0.100 \pm 0.050 \\ \alpha' - \alpha'' &= -0.002 \pm 0.008 \end{aligned}$$

to obtain

$$\begin{aligned} \alpha' &= 0.011 \pm 0.052 \\ \alpha'' &= 0.013 \pm 0.050 \\ \beta &= 0.043 \pm 0.196 \ . \end{aligned}$$

The magnitude of the probabilities indicates that twinning is four times more common than either of the individual stacking faults. Thus, most of the observed line broadening in excess of crystallite size is due to twinning.

2.3. Second moment

The variance, W, of the unfolded diffraction profile is obtained by subtracting the second moment of the reference line from the second moment of the broadened line. That is,

$$W = 2\text{nd } M_c{}^B - 2\text{nd } M_c{}^S \quad (8)$$

W is dependent on the range of ΔS over which the line profiles are examined. $\Delta S = S_2 - S_1$ where $S = 2\sin\theta/\lambda$. An example of the variance obtained as a function of ΔS is given in Fig. 14 for the 111 reflection. For values of ΔS far

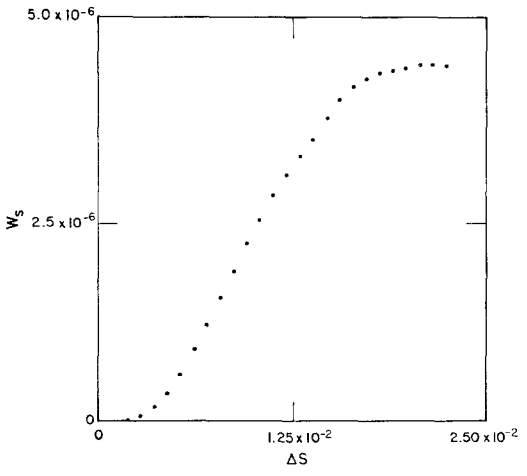

Figure 14 The variance as a function of ΔS for the 111 reflection of a sample of splat-cooled 15Ti–85Pu.

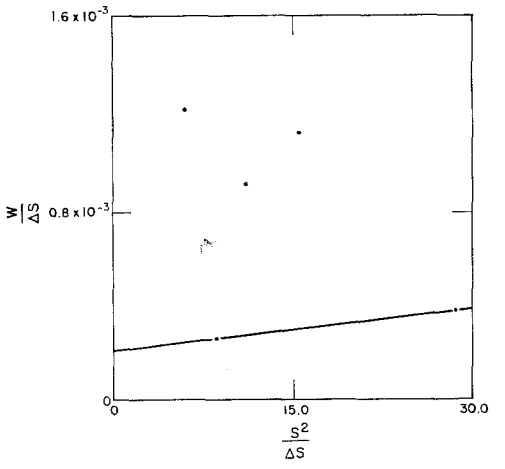

Figure 15 $W/\Delta S$ versus $S^2/\Delta S$ for a sample of splat-cooled 15Ti–85Pu.

beyond the effects of the long tails of the broadened peak W is essentially a constant. As ΔS is decreased and the experimental region of broadening is entered the value of W decreases the decrease being linear in ΔS. For small values of ΔS there is usually a sharp drop in W when the effects of the tails are no longer felt and the value of W approaches zero as ΔS approaches zero. If the intersection of the linear portion and the constant portion of the plot is taken as a measure of the true values of W and ΔS, and this is done for several reflections, then a plot of $W/\Delta S$ versus $S^2/\Delta S$ yields a straight line the intercept of which is equal to $1/2\pi^2 D$ and the slope is equal to (average strain)^2. Values of W and ΔS are given in Table IV. The appropriate

TABLE IV Values of W and ΔS for hkl reflections of splat-cooled 15 Ti–85 Pu

hkl	S	S^2	ΔS (Å^{-1})	W (Å^{-2})
111	0.376	0.142	0.0165	4.149×10^{-6}
200	0.436	0.190	0.0315	38.779
220	0.583	0.336	0.0302	27.454
311	0.724	0.525	0.0338	38.233
222	0.756	0.573	0.0198	7.380

ratios are plotted in Fig. 15. The distribution of points is similar to the plots of integral breadths as a function θ, (see Fig. 5), with the points representing 200, 220 and 311 indicating considerable faulting. The strain determined from the slope of the line through the 111-222 points is 0.0024 and the intercept yields D = 250 Å. Applying this strain to the remaining points yields D = 42 Å for 200, 59 for 220 and 48 for 311.

3. Conclusions

Three different methods of examining X-ray line broadening have been applied to data obtained for a sample of splat-cooled 15Ti–85Pu alloy. The techniques are complementary and all yield essentially identical information.

The integral breadth and variance methods indicate a crystallite size of $\simeq$255 Å and an average strain of $\simeq$0.0030 with considerable stacking faulting evident. The Fourier coefficient method offers the most extensive analysis and the results may be summarized as follows. From an examination of the unfolded Fourier coefficients describing the shape of the diffraction line profile it has been determined that the crystallite size, $D \simeq 260$ Å, the localized strain $\simeq$0.6%, and the combined stacking fault probability $(1.5\alpha' + 1.5\alpha'' + \beta) = 0.078$ while $(4.5\alpha'' + \beta) = 0.100$. From lattice constant variations the combined stacking fault probability $(\alpha' - \alpha'')$ has been determined to be -0.002 as well as the information that the material is under tension. Individual stacking fault probabilities are $\alpha' = 0.011$, $\alpha'' = 0.013$ and $\beta = 0.043$. The reciprocal of the probability is the number of planes of atoms between the indicated stacking fault. The magnitude of the numbers indicates that twinning is four times more common than any other kind of fault.

Acknowledgements

The authors wish to thank Professor B. C. Giessen

for originally suggesting that the analysis should be done and for many helpful discussions. Thanks are also due to Professor B. E. Warren for deriving the form of Equation 3; and to F. W. Schonfeld for his encouragement and support of this research.

References

1. R. O. ELLIOTT, A. M. RUSSELL and B. C. GIESSEN, *J. Mater. Sci.* **8** (1973) 1325.
2. H. P. KLUG and L. E. ALEXANDER, "X-ray Diffraction Procedures" (Wiley, New York, 1954) p. 491.
3. C. N. J. WAGNER, in "Local Atomic Arrangements Studied by X-ray Diffraction", edited by J. B. Cohen and J. E. Hilliard (Gordon & Breach, New York, 1966) p. 219.
4. B. E. WARREN, "X-ray Diffraction" (Addison-Wesley, Reading, Massachusetts, 1969) p. 251.
5. N. C. HALDER and C. N. J. WAGNER, in "Advances in X-ray Analysis", Vol. 9 (Plenum Press, 1966) p. 91.
6. A. J. C. WILSON, *Acta Cryst.* **23** (1967) 888.
7. *Idem, ibid* **A25** (1969) 584.
8. R. B. ROOF, in "Advances in X-ray Analysis", Vol. 15 (Plenum Press, 1972) p. 307.
9. B. E. WARREN, private communication (1973).

Received 8 July and accepted 17 July 1974